Relaxed Fidelity CFD Methods Applied to Store Separation Problems

Rudy Johnson
AFRL/VAAI
2130 Eighth St.
WPAFB, OH 45433

Rudy.Johnson@wpafb.af.mil

M. Bruce Davis
Lockheed Martin Aeronautics
P.O. Box 748
Fort Worth, TX 76101

Myron.B.Davis@lmco.com

Dennis Finley
Lockheed Martin Aeronautics
P.O. Box 748
Fort Worth, TX 76101

Dennis.B.Finley@lmco.com

ABSTRACT

The goal of relaxed fidelity computational fluid dynamics (CFD) methods is to provide a store separation analysis capability that lies between the accuracy-productivity characteristics of influence function methods and time-accurate CFD methods. Two methods are presented in this paper, both of which provide significant accuracy improvements over influence function methods while providing rapid enough turn around times to support parameter and design studies. The first technique discussed is the Minimized Domain CFD (MDCFD) method. This method allows the collection of store force and moment data on relatively small 'minimized' domains that contain the store of interest and any other nearby geometry. The boundary conditions on the minimized domain are extracted from a baseline CFD solution of the full aircraft configuration. The product of the MDCFD method is a set of store force and moment coefficients at various locations relative the aircraft. This method is demonstrated on the Miniature Munition Technology Demonstrator (MMTD) and the Powered Low Cost Autonomous Attack System Tandem Pack Configuration (PLOCAAS) in the flow field of the F/A-22 aircraft. Force, moment, and trajectory predictions are compared to $1/15^{th}$ scale wind tunnel data. The second technique discussed is the Sensitivity Analysis (SA) method. In this method sensitivity derivatives are computed from a baseline CFD solution on a store using a linearized perturbation scheme and these sensitivity derivatives are added to the baseline solution to obtain the new flow field. The resulting solution costs significantly less to compute than the original baseline solution and allows the efficient computation of a parameter space around a specific baseline solution. The method presented applies perturbation boundary conditions at the surface of the store for variations in store orientation. Predictions are made for a one-degree change in angle of attack and angle of sideslip for the MMTD and PLOCAAS to demonstrate this capability.

1   INTRODUCTION

The intent of the aircraft-store certification process is to ensure safe carriage and separation within the aircraft flight regime. Typically the store/aircraft/flight condition is evaluated using a combined analysis. This involves comparison to previously cleared stores in a similar configuration, computational fluid dynamics (CFD) analysis, wind tunnel testing, and actual flight tests when necessary. Only limited flight tests are accomplished at critical conditions due to expense, test aircraft availability, and risks to the pilot. Wind tunnel testing is used to demonstrate safe separation characteristics by gathering grid matrix data and captive trajectory system (CTS) data for trajectory analysis. Wind tunnel testing, although less expensive than flight testing, is still expensive, and reliable analysis techniques that reduce wind tunnel time would correspondingly reduce cost. The introduction of computational fluid dynamics (CFD) into the aircraft-store certification process has held great promise as a method to reduce test requirements and accelerate the certification

		Form Approved
Report Documentation Page		OMB No. 0704-0188

Public reporting burden for the collection of information is estimated to average 1 hour per response, including the time for reviewing instructions, searching existing data sources, gathering and maintaining the data needed, and completing and reviewing the collection of information. Send comments regarding this burden estimate or any other aspect of this collection of information, including suggestions for reducing this burden, to Washington Headquarters Services, Directorate for Information Operations and Reports, 1215 Jefferson Davis Highway, Suite 1204, Arlington VA 22202-4302. Respondents should be aware that notwithstanding any other provision of law, no person shall be subject to a penalty for failing to comply with a collection of information if it does not display a currently valid OMB control number.

1. REPORT DATE **01 JUN 2004**	2. REPORT TYPE **N/A**	3. DATES COVERED **-**	
4. TITLE AND SUBTITLE **Relaxed Fidelity CFD Methods Applied to Store Separation Problems**		5a. CONTRACT NUMBER	
		5b. GRANT NUMBER	
		5c. PROGRAM ELEMENT NUMBER	
6. AUTHOR(S)		5d. PROJECT NUMBER	
		5e. TASK NUMBER	
		5f. WORK UNIT NUMBER	
7. PERFORMING ORGANIZATION NAME(S) AND ADDRESS(ES) **AFRL/VAAI 2130 Eighth St. WPAFB, OH 45433**		8. PERFORMING ORGANIZATION REPORT NUMBER	
9. SPONSORING/MONITORING AGENCY NAME(S) AND ADDRESS(ES)		10. SPONSOR/MONITOR'S ACRONYM(S)	
		11. SPONSOR/MONITOR'S REPORT NUMBER(S)	
12. DISTRIBUTION/AVAILABILITY STATEMENT **Approved for public release, distribution unlimited**			
13. SUPPLEMENTARY NOTES **See also ADM201999., The original document contains color images.**			
14. ABSTRACT			
15. SUBJECT TERMS			

16. SECURITY CLASSIFICATION OF:			17. LIMITATION OF ABSTRACT **UU**	18. NUMBER OF PAGES **26**	19a. NAME OF RESPONSIBLE PERSON
a. REPORT **unclassified**	b. ABSTRACT **unclassified**	c. THIS PAGE **unclassified**			

Standard Form 298 (Rev. 8-98)
Prescribed by ANSI Std Z39-18

process. Unfortunately this has not materialized due to the time required to obtain reliable CFD results in the quantity necessary to support the store separation analysis process.

The idea behind the computational methods documented in this report is to provide sufficiently accurate aerodynamic force and moment coefficients while reducing the time required to generate the necessary aerodynamic data. Considering productivity, accuracy, and complexity as three parameters in the model conceptual space, which encompasses aerodynamic prediction methodology, production is seen to decrease as model accuracy is increased (Figure 1).   Typically, simplified computational approaches such as influence function methods are capable of rapid analysis and support high productivity, but their accuracy for complex geometries is suspect. At the other extreme highly detailed time-accurate CFD methods can produce very accurate results but since the computations are so time-consuming productivity drops significantly. The goal of the relaxed fidelity CFD is to generate store force and moment data more quickly than full featured time-accurate CFD while maintaining sufficient accuracy to be useful for separation analysis.
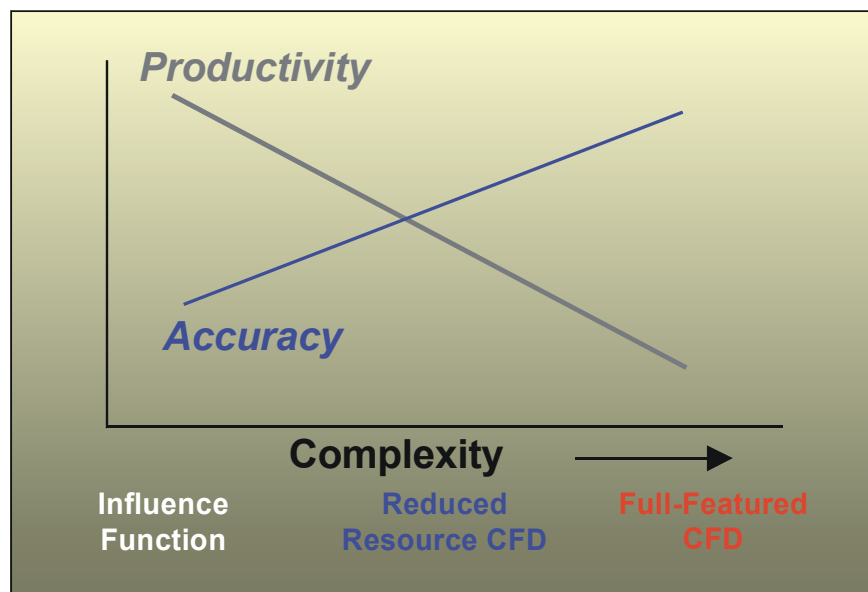

Figure 1: Accuracy/Fidelity Spectrum For CFD Methods

Having established the premise for reduced fidelity model development an outline of the approach can then be put forth. The details of the MDCFD method, including methods to obtain time-averaged (or steady state) solutions, how to account for mutual interference effects, and general guidelines for application of MDCFD are discussed in the next section. In the Sensitivity Analysis (SA) section a method is described for the computation of store loads due to local variation in store orientation relative to an existing CFD solution. The details of the application of sensitivity derivatives to compute perturbation solutions and the application of local surface boundary conditions are discussed. In the fourth section results are presented for the two methods. The MDCFD method is used to compute loads on two 250-pound stores (the MMTD and PLOCAAS Tandem Pack) in proximity of the F/A-22 aircraft. MDCFD results are compared to baseline CFD loads as well as 1/15 scale wind tunnel data. The SA method is demonstrated on the MMTD and PLOCAAS Tandem Pack geometries in free stream conditions. Results are compared to full CFD results for changes in angle of attack and angle of sideslip.

2   MINIMIZED DOMAIN COMPUTATIONAL FLUID DYNAMICS METHOD

The minimized domain CFD (MDCFD) approach may be simply described as a subset domain used to solve a flow field within a minimum volume of interest. This method may be applied to store separation simulation by first generating an aircraft flow field solution without the store of interest present. The next step is to define a near field domain containing the store of interest, the portion of the aircraft near the store, and any carriage equipment or other stores that are close by. The near field domain should be large enough to contain any local unsteadiness (such as the weapons bay) and be large enough to allow the store to progress away from any strong mutual interference with the aircraft and other equipment. In the near field domain the store is moved relative to the fixed aircraft geometry while the domain itself remains fixed relative to the aircraft. The domain outer boundaries need to be far enough from the store such that instabilities are not introduced due to the boundary requirements. Once the near field domain is defined the boundary condition information at the outer edge of the domain is interpolated from the time averaged full aircraft solution.

An additional domain, referred to as the far field domain, is usually defined to collect store load data beyond the near field domain. With the far field domain the store domain is moved for each new store position while the store remains fixed relative to the domain and the interpolated boundary conditions are extracted each time. The far field domain is far enough from the aircraft that no aircraft hardware or other stores are included in the domain, allowing the domain to be smaller and contain fewer points than the near field domain, yielding additional savings.

Now that the boundary conditions are set a CFD solution is obtained for the minimized domain. This allows only one full aircraft solution while the store may be located at several positions in the near field domain and the solution for each location can be computed independently. The net effect is the ability to generate a database of store force and moment data as a function of store location for use by a six degree of freedom simulation. This is essentially the computational equivalent of the data collected during the grid-testing portion of a wind tunnel test.

It should also be noted that the store of interest may be swapped out and the procedure repeated to produce loads on multiple stores from the same full aircraft solution. This procedure when applied appropriately results in surprising accuracy for the test cases studied. An approach like this allows for the solution of tens of store locations overnight on a workstation class computer. For the time averaged flow field approach chosen here for unsteady problems, the aircraft solution can be used to produce many store solutions with this "frozen" flow field, or one-way interface, approach. If mutual flow field interference effects are important, the aircraft solution could be updated periodically to provide two-way interaction. Such an approach would require more computational resources.

### 2.1   Application to the F/A-22 and MMTD store

The application selected to demonstrate the MDCFD approach is the separation of the MMTD from the right main weapons bay of the F/A-22 aircraft. The geometry used to generate the full CFD solution on the F/A-22 is shown in Figure 2. This geometry without the tails was selected to match the 1/15th scale wind tunnel model used to generate the data that will be used for evaluation of the MDCFD method.
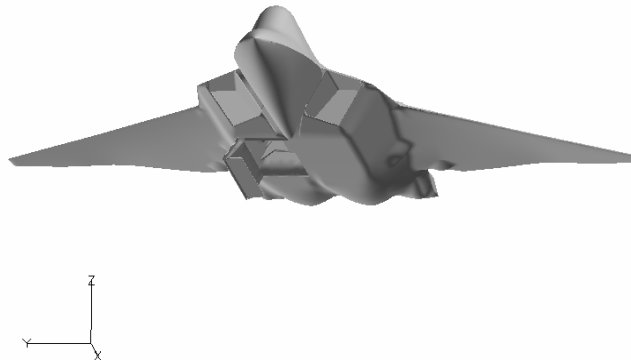
Figure 2: V-11 wind tunnel model of F/A-22 with right main weapons bay open

As seen in Figure 3, the near-field minimized domain includes the weapons bay as well as significant area surrounding the bay. The minimized domain also extends well down from the bay, and in fact dwarfs the MMTD. The purpose of the large domain is to maintain a large enough area that the unsteady flow in and immediately around the bay can be allowed to develop, and to place the interface boundaries as far from the bay as possible so that the effects of a steady interface can be mitigated. In Figure 3 the bay doors, the spoiler and the MMTD are shown in magenta to give some idea of the extent of the minimized domain. It is obvious that a smaller domain could easily accommodate the MMTD as well as the entire bay. The geometry for a far-field domain was generated as well, and is shown on the right side of Figure 3. This geometry is somewhat trivial, however, since it is merely a rectangular box. Again, it is evident that a smaller box could easily contain the MMTD within the accuracy limits of the minimized domain method.
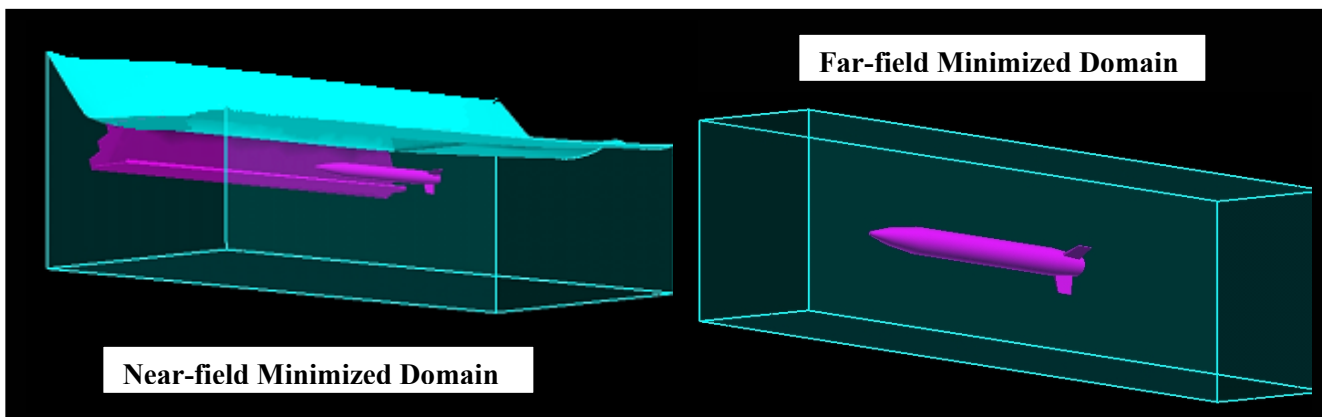
Figure 3: Near-field and far-field minimized domains with MMTD shown for scale

In the near-field minimized domain the MMTD is moved to each new location and a new grid is generated by the mesh generation capability within Splitflow. The near-field domain outer boundaries remain fixed such that the boundary conditions interpolated from the full aircraft solution remain the same. For the far-field minimized domain the domain itself is positioned with the store and new boundary condition information is interpolated from the full aircraft solution at each store/domain location. The store movement process is fully

automated and once the store locations are input each minimized domain solution proceeds independently. The independent nature of the simulations allows perfectly parallel simulations

2.2   Approach to Treating Unsteady Flow

As mentioned earlier the approach is to obtain a time-averaged or "steady" CFD solution for the full aircraft. This presents a problem since the weapons bay aerodynamics are inherently unsteady even for the inviscid flow models. There are four ways to handle the unsteadiness between the aircraft flowfield solution and the MDCFD solution:

> 1. Resolve the unsteadiness in both the aircraft flowfield solution and the MDCFD solution. The plot files for the flowfield solution need to be saved for a full cycle of the shear layer (or the lowest frequency phenomena of importance) at each time step, and these plot files are used to extract time-dependent interface boundary conditions for the minimized domain.

> 2. Treat the aircraft flowfield solution as unsteady and resolve the time dependence, but time-average the MDCFD solution. Interface boundary conditions would be time-dependant, but the solution itself would be time-averaged.

> 3. Time-average the aircraft flowfield solution but resolve the unsteadiness in the MDCFD solution. The interface boundary conditions would be steady but the interior solution would be run time-accurate and instabilities allowed to develop.

> 4. Time-average both the aircraft flowfield solution and the MDCFD solution.

The first and second options would involve saving a massive amount of data from the aircraft flowfield simulation in the form of plot files at each time step. This violates the spirit of the MDCFD method, which is to reduce the required resources for store loads calculation and is not considered further. Time-averaging the aircraft flowfield solution seems to be the best option and allows either of the third and fourth options, and hence time-averaged or steady aircraft flowfield solutions will be used for the rest of this study. The full time-accurate solution can be allowed to develop in the MDCFD solution with the interface boundary conditions held constant. The key here, as mentioned previously, is to construct a minimized domain large enough such that the unsteady phenomena are primarily restricted to the minimized domain itself.

3   SENSITIVITY ANALYSIS METHOD

The second relaxed fidelity method to be investigated is the Sensitivity Analysis (SA) method. The application of sensitivity analysis to CFD codes provides a way to create linearized estimates of the effects of changes in geometry or flow condition on the non-linear flowfield (References 3-5). This allows rapid assessment of small changes in surface shape, angle of attack, or Mach number without reconverging an entire flow domain. In concept, the sensitivity approach uses information from a reference solution to solve for flow derivatives in each computational cell. These derivatives are developed relative to the parameter of interest in a 'chain-rule' manner from the governing flow equations. This results in a linear set of equations to be solved for flow derivatives in each cell. A perturbation approach is used to develop the sensitivity equations and boundary conditions.   This research is still in progress (Reference 6); the methodology produces a computational model that is similar to that of Reference 3. The Splitflow CFD solver at LM Aero is used as the framework for the sensitivity derivative solver, and a Splitflow solution is used for input of the grid and baseline solution in each cell. The sensitivity derivative solver finds the derivatives of the Euler equations due

to each flow parameter. The boundary condition for the sensitivity with respect to a given parameter combines geometric effects of the parameter on the velocity components with characteristic-based projection of pressure and temperature perturbations to create a closed-form solution at the domain boundaries. A set of derivatives can be generated in each computational cell with respect to each of several variables, then these derivatives can be combined together using superposition and added to the baseline data to produce the estimated flowfield. The cost of each sensitivity solution for the current method is on the order of 20% to 50% of the original flow convergence. The current method uses the existing Splitflow implicit solution technique, and no attempts have been made to increase convergence speed for this linear set of equations. Further research is needed to determine the level of performance that can be achieved.
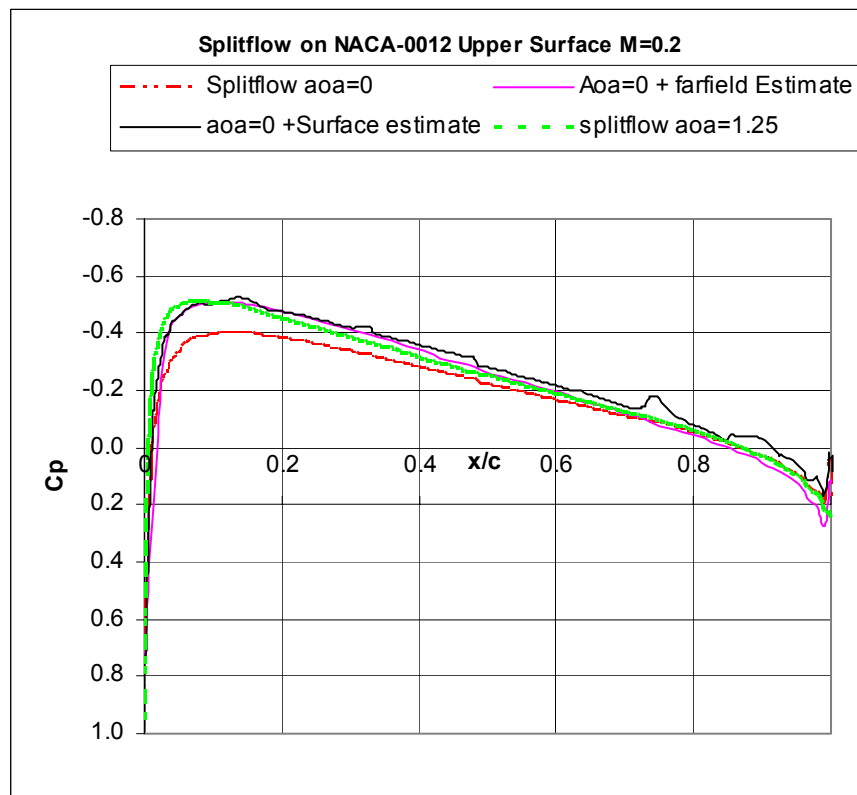
Figure 4: Perturbation pressure comparisons between farfield boundary condition and surface boundary condition for NACA 0012 airfoil at Mach 0.2

4   RESULTS

In this section results are first presented for the MDCFD method applied to a full aircraft/store configuration. The resulting store loads are used to generate trajectory estimates and comparison is made to experimental data.   After the MDCFD are discussed application of the SA method to the PLOCAAS Tandem Pack and MMTD geometries in free stream flow conditions are examined.

4.1   MDCFD Results

The MDCFD method is applied to the MMTD with fins deployed and the PLOCAAS Tandem Pack in proximity to the F/A-22 aircraft at Mach numbers of 0.9 and 1.3. The computed store loads are discussed relative to baseline CFD results and wind tunnel captive grid loads data. Details of a grid study performed on the minimized domains to look at domain size and grid dependence of the solution are summarized. Then computational force and moment data is input into a six degree-of-freedom code to analyze the trajectory of both stores from the aft carriage position in the right main weapons bay and to compare to wind tunnel captive trajectory system (CTS) data.

4.1.1   Loads Data

In order to compare the MDCFD generated force and moment data to fully featured CFD loads twenty baseline cases are run. These baseline solutions are computed at Z-locations of 0, 0.5, 1.9 (approximate shear layer location), 4 and 8 feet below the aft store carriage location in the F/A-22 right main weapons bay for both stores and both Mach numbers. These solutions are inviscid and first order in space. With the first order spatial approximation the solutions converge to steady state due to the artificial dissipation of the method, thus avoiding the need to average forces and moments. The resulting force and moment data for these solutions are labelled "CFD Baseline" in Figures 5-8.

The MCFD computations begin with computation of an aircraft influence flow field (the full aircraft without the store of interest). As discussed earlier a time-averaged or steady state aircraft influence flow field is needed to interpolate boundary condition information for the minimized domains. This is accomplished by converging first order solutions to steady state. There are only two aircraft influence flow fields generated, one at Mach 0.9 and the other at Mach 1.3, since the simulated release hardware for both stores was the same.

With the aircraft influence flow fields complete the next step is to choose how the solution will be computed on the minimized domains.   Three variations are examined. First the minimized domain solutions are computed first order, which results in steady loads. Second the minimized domain solutions are computed second order accurate with time warping[1] and the loads are averaged over enough iterations to get a meaningful average. In the third method the solutions are computed time accurate and second order in space and again averaged over a sufficient number of iterations. The time step used is $2x10^{-5}$ seconds, which was used for acoustic simulations in a previous program on the same geometry, and is thought to be adequate for the purposes here.

The MDCFD force and moment data is plotted in Figures 5-8 along with the baseline CFD and wind tunnel data. The first order near-field results are labelled "Min Domain NF" and the far-field results are labelled "Min Domain FF." The second order time warped results are labelled "MD 2nd order NF" and "MD 2nd order FF." The time accurate second order solution for the near-field domain is labelled "MD time acc NF". No time-accurate solutions are computed for the far-field domain since the boundary conditions are steady and there is nothing contained in the domain to cause unsteady flow. The wind tunnel data is plotted with error bars in the figures. There is no axial force data for the MMTD wind tunnel test results since a five-component balance was used during the test.

In the interest of brevity, there is a significant amount of data condensed into Figures 5-8.   In order to evaluate the MDCFD approach three details are examined. The first is how well MDCFD matches the baseline CFD results. Second is how well does the MDCFD reproduce the wind tunnel loads data. And the third is when to switch from the near-field domain to the far-field domain solution.

The first item of comparison is the MDCFD results with the baseline CFD. If MDCFD introduces no error in the solution the first order near field and far field solutions would match the baseline results exactly. Recall we are not trying for an exact match only to more efficiently generate the loads data, so exact matches in magnitude are not expected. It is expected that the magnitudes will be close and in most cases they are no worse than the baseline results relative to the wind tunnel data. Consistently capturing the trends and demonstrating comparable accuracy is more important.   The first order MDCFD axial forces definitely indicate the same trend as the baseline CFD but uniformly indicate reduced force magnitudes (especially for

---

[1] The solution is advanced by a local value of the time step computed from the global CFL condition. This method of convergence acceleration is also referred to as local time stepping in the literature.

the MMTD). The PLOCAAS results seem to indicate that this may mean that the MDCFD results are more accurate, possibly due to reduced artificial dissipation near the body. The rolling moment results are small but do indicate differences within the bay. The values are so small that they are almost all within the error bands of the wind tunnel values. Outside of the bay the match is good except for the supersonic PLOCAAS at z=-8, and this is so far from the other results that the validity of this value must be considered suspect. Side force and yawing moments also show disagreement within the bay and match better when the store is out of the bay. The MDCFD side force coefficients are slightly larger for all cases relative to the baseline and the yaw is consistently near zero. The normal force on the far-field domain compares well with the baseline, however the near-field results do not. The pitching moment compares well to the baseline, except for the supersonic PLOCAAS case mentioned previously.

The second order MDCFD results reduce the axial forces as would be expected from the reduced dissipation of the numerical method.   The second order results in general also compare better to the wind tunnel data than the first order baseline and MDCFD. The exception is the bulge in the supersonic side force, normal force, yaw and pitch seen in the wind tunnel data. This is thought to be the effect of a wing-mounted pod on the wind tunnel model that was not modelled in the CFD cases. For the Mach 0.9 subsonic/transonic case this causes a flow disturbance, which does not seem to affect the flow significantly in the vicinity of the weapons bay. However, in the supersonic case, there is a shock originating at the nose of this pod, and it apparently crosses the path of the store. Overall the comparison with wind tunnel data with the second order MDCFD is reasonable.

The comparisons for the second-order simulations reveal several general trends. The most important is that the second-order time-warped simulations are almost uniformly more accurate than the first-order.   The average loads obtained from the time-accurate simulations seemed to be no better, and in some cases actually worse, than the same time-warped simulation. This would tend to eliminate from consideration the use of time-accurate simulations given the much larger computational time for such simulations. This is not surprising given that the goal is simply the average loads. These results suggest that to obtain average loads for internal weapons bay release problems, it is best to average a second-order time-warped solution rather than use the first-order solution or average a time-accurate solution. The second-order MDCFD simulations seem to match the wind tunnel data better than the first-order CFD baseline simulations, again almost uniformly. CFD baseline simulations were not performed second-order, which would perhaps be a fairer comparison. In general, however, MDCFD seems to be comparable to full CFD in terms of accuracy.

In order to assess when to switch MDCFD solutions from the near-field domain to the far field domain loads are calculated with the MMTD located 4 and 5 feet below the aircraft using both domains. Ideally the loads would be the identical on either domain, and any differences indicate inaccuracy introduced by one of the minimized domain problems. Differences in this region may be a result of the mesh limitations as the store approaches the bottom of the near-field boundary. Examination of this overlap region in Figure 5 shows that for axial force, rolling moment and yawing moment, the values at z=4 show good agreement, indicating that this is a good place to transition the data from one domain to the other. The side force shows good agreement at z=5, indicating that this is a good transition point. For these coefficients, then, the best strategy seems to be to use the near-field domain value at z=4 and the far-field value at z=5. The normal force and pitching moment coefficients present a completely different story. Not only are the values very different, but the trends in the overlap region between the two domains are different as well. To adequately capture the coefficients in this overlap region the near-field region may have to be extended significantly downward such that the overlap region is much larger. Averaging the coefficients at one of the overlap locations seems to give a value close to the wind tunnel value, but there is no theoretical reason why this would be so.

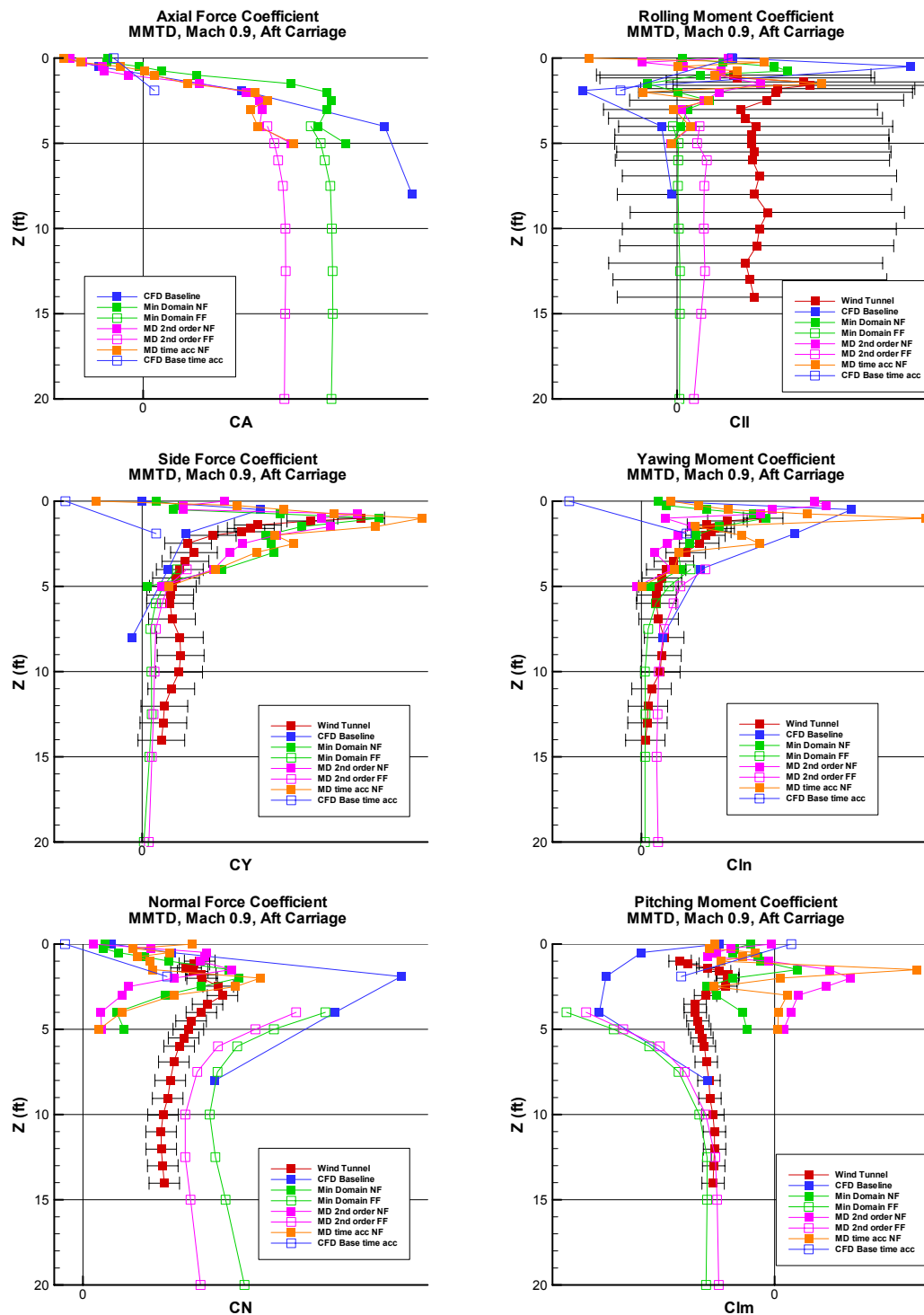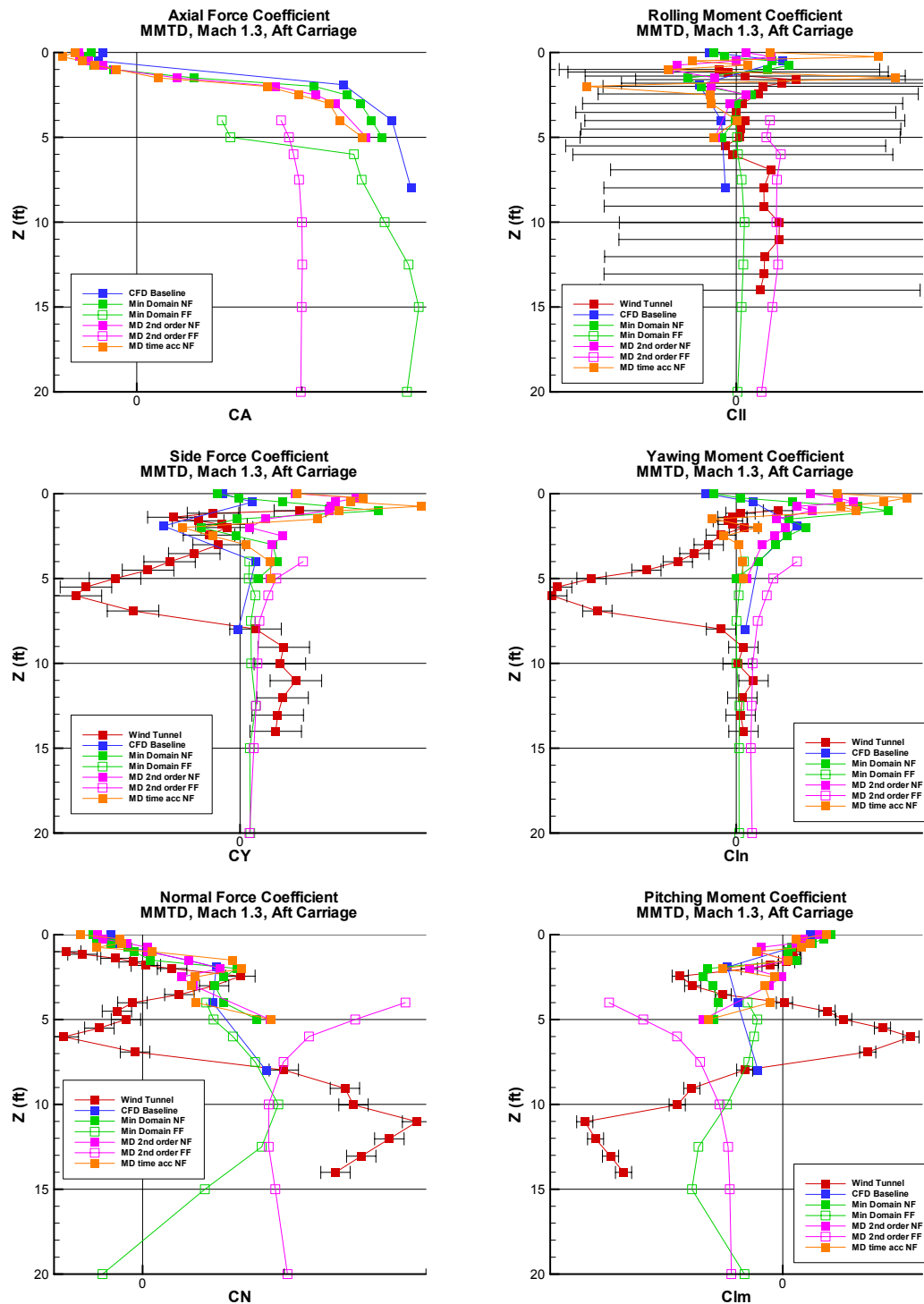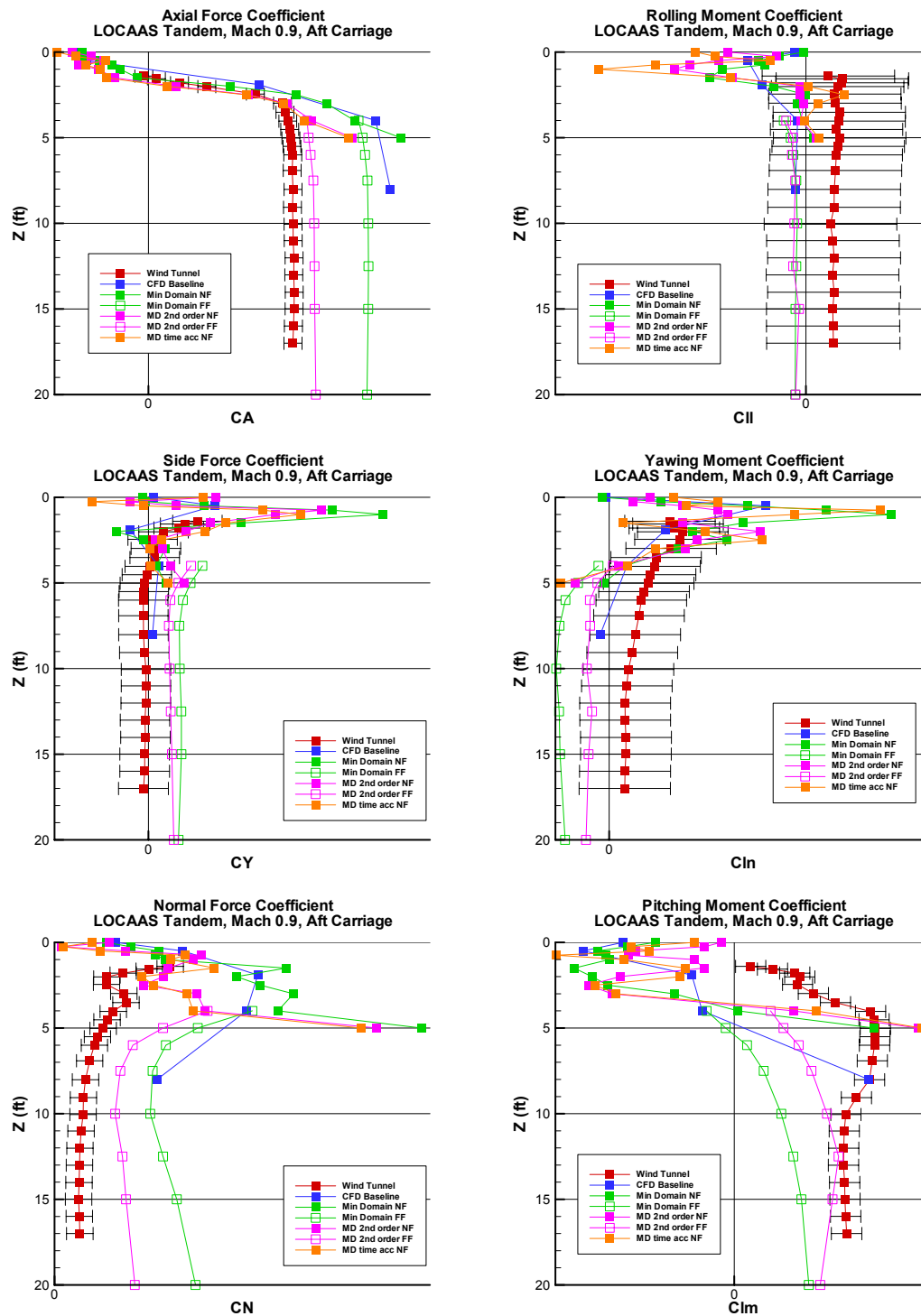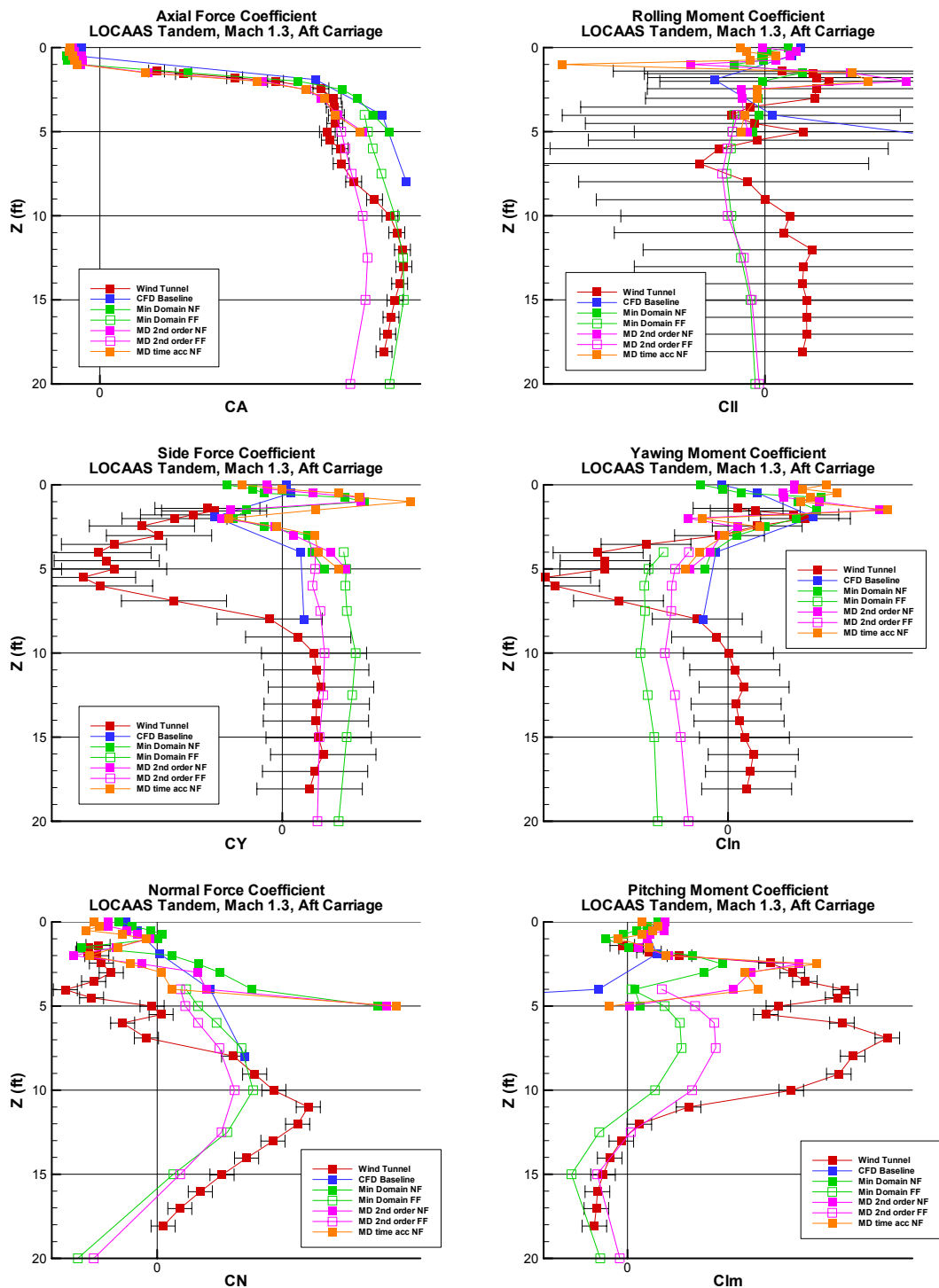**Figure 5: Loads comparison, MMTD, Mach 0.9, aft carriage**

Figure 6: Loads comparison, MMTD, Mach 1.3, aft carriage

Relaxed Fidelity CFD Methods Applied to Store Separation Problems

Figure 7: Loads comparison, LOCAAS, Mach 0.9, aft carriage

Figure 8: Loads comparison, LOCAAS, Mach 1.3, aft carriage

4.1.2   Grid Study

As part of the effort to determine the accuracy of the MDCFD method a two part grid study was undertaken. First, for a given minimized domain, the number of cells in the domain is varied and the loads recorded to see if the calculated loads were grid dependent. Second, two different domain sizes were tried to see how the accuracy varied with the domain size for the same number of cells. Since the near field domain was considered to be large (certainly as compared to weapon size) a small near field domain was constructed which was smaller in every dimension by about 1/3. The far field minimized domain was of nominal size, so a larger far field domain was constructed, which was larger by a factor of two in every dimension. The number of cells in the previous simulations was 300,000 cells for the far field domain and 400,000 cells for the near field. For each minimized domain, one total cell number below this value and two above this nominal value were computed and the loads extracted.

Comparison of the large far field domain shows almost identical values for grids ranging from 200,000 cells to 500,000 cells, indicating grid independence of the loads. The large near field results show almost identical results for all grids except the 700,000-cell case, which is consistently different than all of the other grid sizes and compares worse with the wind tunnel data, which casts some doubt on its validity. The same study for the smaller domains show that both the near field and far field domain comparisons are virtually identical, indicating grid independence has been achieved for both domains.

Given the grid independence exhibited for both the large and small domains, the large and small domains were compared to one another at the previous nominal grid sizes. The far field domain shows almost identical results between the domains, with slight differences in axial force, normal force, and pitching moment (on the order of 5%). These results are computed first-order, so the small differences are not surprising, and are insignificant compared to the difference in first and second-order results. The near field domains have a more profound difference. The small minimized domain yields loads which are far different from the larger domain, and consistently worse as compared to wind tunnel data. This would seem to justify the choice of a large minimized domain in the near field of the weapons bay.

The conclusion from the grid studies is that in the range of cell sizes that were used in this study (300,000 grid cells), the solution is independent of grid size. The loads calculation also seems to be insensitive to the size of the far field domain where the width of the domain is approximately 40% of the length of the store, which is a compact minimized domain. The solution is sensitive, however, to the size of the near field domain, and it seems to be important to construct a domain which is of sufficient size to contain the unsteady effects immediately surrounding the bay.

4.1.3 Trajectory Predictions

The store loads computed by the minimized domain method result in a data set which approximates the grid loads generated during wind tunnel testing. Trajectories are computed from the first order MDCFD loads data using a six degree-of-freedom trajectory simulation code and compared with the wind tunnel CTS trajectories. Trajectory calculations have not been performed for the CFD baseline loads or for second-order data.

Figure 9 and Figure 10 show the trajectory comparisons for the MMTD and PLOCAAS Tandem Pack. Excellent agreement in the Z trajectory and good agreement for the X and Y trajectories is evident. Comparison of the pitch and yaw angle (roll angle was considered irrelevant since the rolling moment was so small) is not very good for either flow condition and may be attributable to the differences in computed and experimental moment coefficients within the bay. Outside of the bay the moment coefficients are small for both experimental and computation.
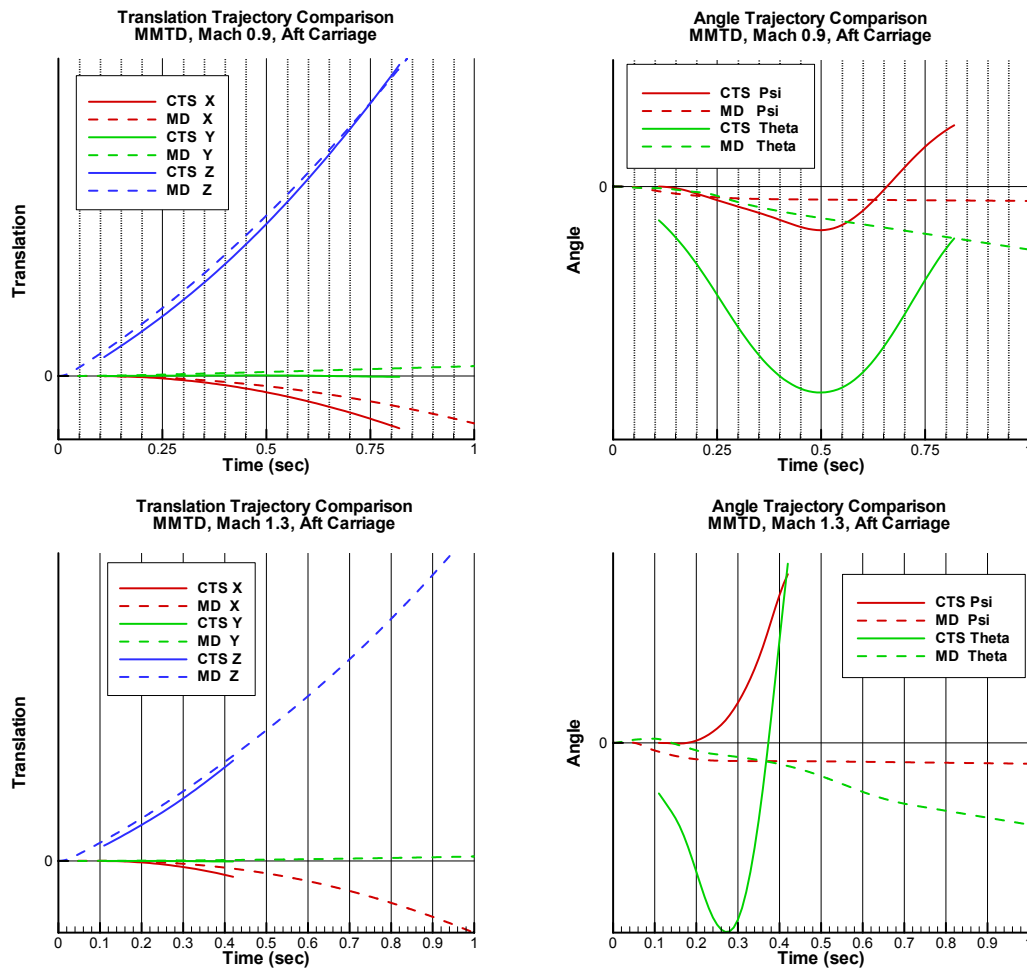
Figure 9: MMTD aft release trajectory comparison at Mach 0.9 (top) and Mach 1.3 (bottom)
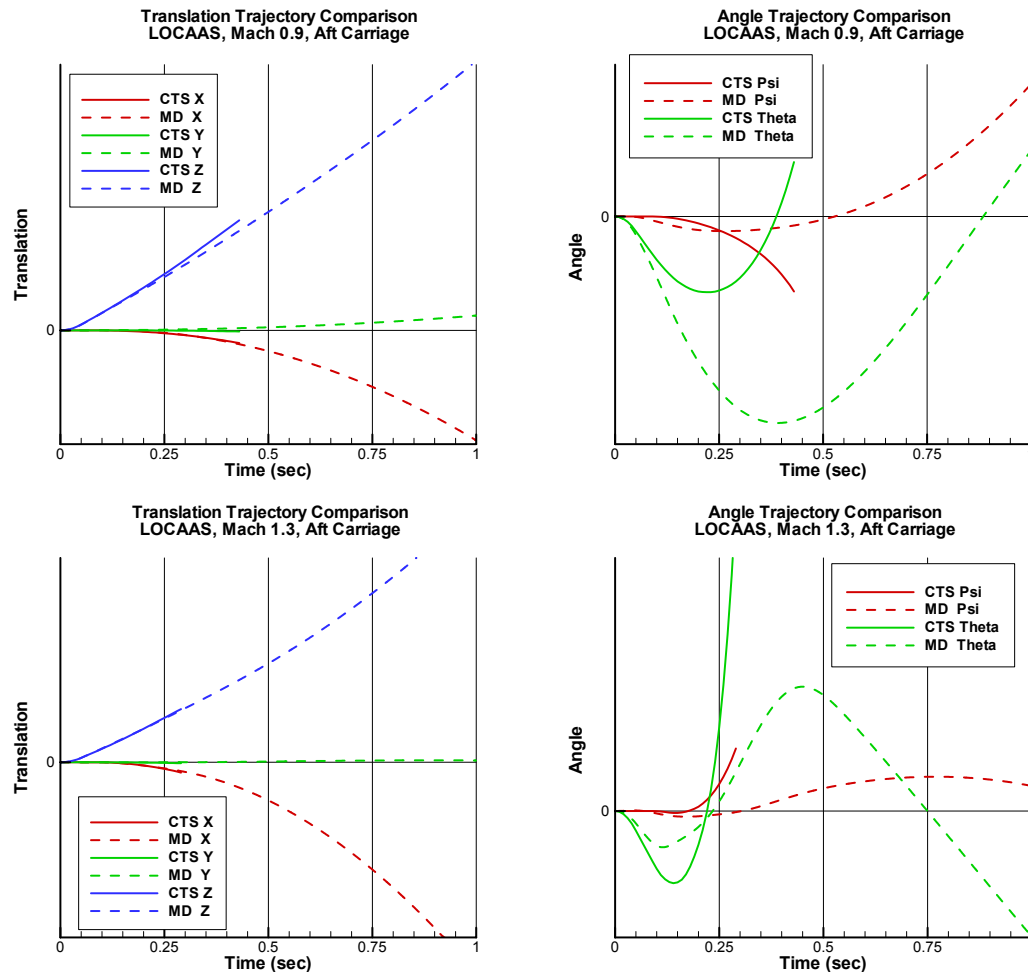
Figure 10: PLOCAAS aft release trajectory comparison at Mach 0.9 (top) and Mach 1.3 (bottom)

4.1.4 Summary of the MDCFD Method Results

The MDCFD method performed as well on internal release problems as it did on external release problems. That is, the comparison between MDCFD, full CFD, and test data showed no clear trend to increased accuracy with solver complexity. This is true of the first-order MDCFD as well as second-order MDCFD. In fact, if there is any trend, it suggests that the second-order time-warped averaged loads are more accurate than the first-order full CFD loads. Although the test data did not extend all the way to carriage for sting interference reasons, the predicted loads seem to be slightly less accurate in the aggregate than the far field results. The second-order MDCFD is definitely more accurate than the first-order simulations. This is true not only of axial force, but of the other force components as well. The obvious suggestion is that second-order time-warped simulations be performed and the loads averaged from the iterate data. The grid study indicates solution grid independence on domains of the same physical size. Variation of the actual physical size of the minimized domain indicates that the near field domain should be large enough to contain the unsteady flow.

Trajectories predicted from the first order MDCFD loads data agree well with location but fail to reproduce the angular orientation data collected in the wind tunnel. The angular variations are not large enough to significantly affect the trajectory, and the ability to predict safe separation is unaffected by the differences.

4.2   Sensitivity Analysis Results

The SA method is applied to compute unit changes in angle of attack and angle of sideslip for both the MMTD and the PLOCAAS Tandem Pack. The flow conditions used to evaluate the MDCFD method are also used to evaluate the Sensitivity Analysis method. However, the SA solutions are performed on the store alone in the freestream, and not in the flowfield of the aircraft. This was deemed adequate to evaluate the method itself at the current exploratory stage of development.

4.2.1   PLOCAAS Results

The perturbation pressure coefficient and velocity vectors for unit variation in angle of attack (from a baseline of zero alpha) are shown in Figure 11. The perturbation pressure results (left side of figure) indicate areas of pressure change which would be expected for a store at angle of attack. The lower part of the nose region of the LOCAAS near the leading edge experiences perturbation increments greater than zero, while the upper surface experiences a decrease. The perturbation velocity vectors are also as expected. The region below the nose is at unit angle (positive nose up) and hence the net change in velocity is downward, corresponding to the pressure rise. On the upper surface, a large upward directed perturbation is caused by the discontinuous break in slope. This qualitatively would induce velocity increments similar to the effect of significant flow expansion or separation at the sharp corner.
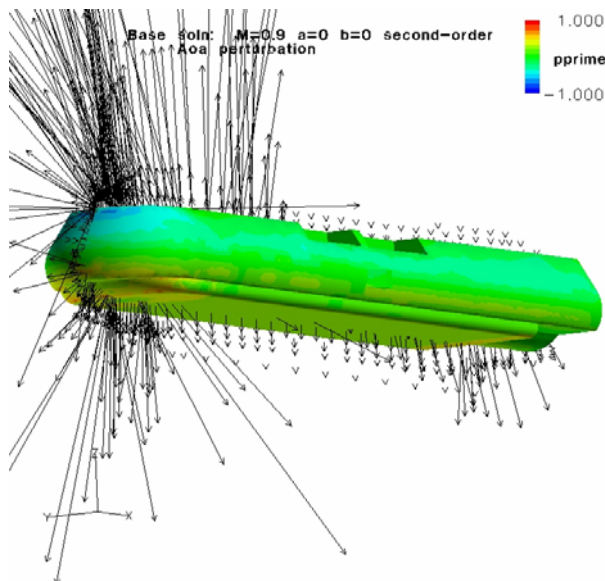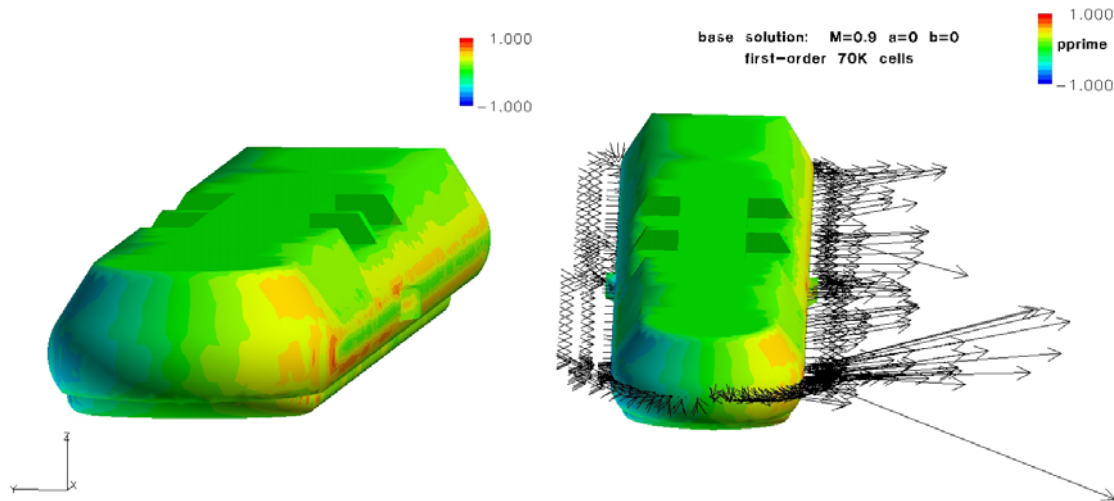

Figure 11: Perturbation pressure coefficient and velocity vectors with angle of attack, LOCAAS, Mach 0.9

Similar results for unit change in the angle of sideslip are shown in Figure 12. The results are slightly different than for angle of attack change. The front of the LOCAAS has a smoother transition in the lateral direction from the front to the sides, so there is no flow separation and the velocity change on the leeward side is in the direction of the store, matching the angular change of the body. Again, large velocity changes on the windward side correspond to the change in angle of the surface. The pressure results are as expected, with perturbation pressure greater than zero on the windward side and less than zero on the leeward side.

Figure 12: Perturbation pressure coefficient and velocity vectors with angle of sideslip, LOCAAS, Mach 0.9

The perturbation pressure and velocity vectors with angle of attack and sideslip for the LOCAAS at Mach 1.3 are shown in Figure 13 and Figure 14. In general behavior, the results are similar, but there are several key differences. First, the LOCAAS at this Mach number seems much less sensitive to changes in both angle of attack and sideslip. This is probably due to the presence of a bow shock in front of the LOCAAS at this Mach number, reducing the sensitivity behind the shock. The lower energy flow does not separate over the leading lip upper edge, and hence no upward velocity perturbations are present there. The velocity perturbations with beta on the windward side are almost uniform in strength corresponding to a uniform pressure increment along the body side.
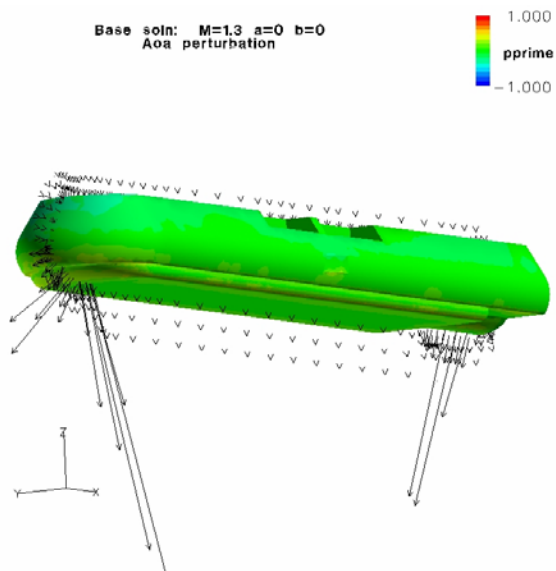
Figure 13: Perturbation pressure coefficient and velocity vectors with angle of attack, LOCAAS, Mach 1.3
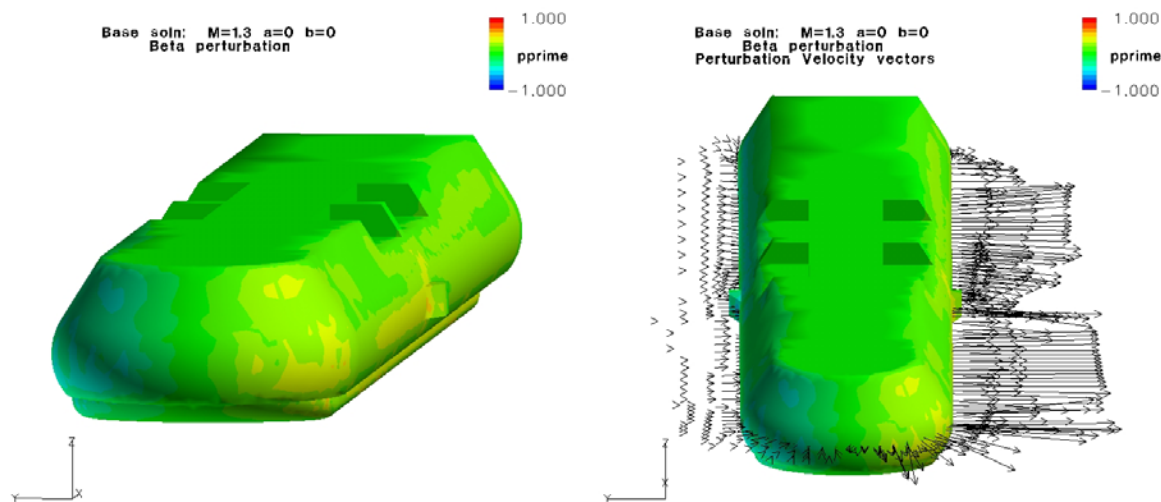

Figure 14: Perturbation pressure coefficient and velocity vectors due to sideslip, LOCAAS, Mach 1.3

The unsteadiness of the flow using a second-order accurate solver was described in a previous section. This is especially evident for the LOCAAS geometry which has geometric features which cause significant regions of unsteady flow. When the SA solver was run using baseline flowfields of first-order and second-order, the resulting perturbation solution indicated substantial variation with grid resolution. The starting grids which had more uniform pressure fields generated better perturbation results. The conclusion to be drawn is that a

steady flow is required as a starting point for sensitivity calculations, even if a reduced resolution is necessary to achieve the steady prediction.

Store loads were computed using both full CFD (Splitflow) and the SA method. The SA flow derivatives were computed using a zero-aoa and zero-beta base solution. The estimated force/moment at angle of attack or sideslip was computed by multiplying the perturbation cell-center data by the selected angle of attack or sideslip and adding it to the base solution at zero orientation, then integrating the resulting surface pressures. Figure 15 shows the sensitivity results with angle of attack at Mach 0.9 for the LOCAAS. Experimental data was not available for this geometry, and the coefficient axes shown for LOCAAS are qualitative in nature. Both the full CFD and the perturbation estimates were performed using first-order and second-order accuracy. The first-order perturbation estimates seem to match the second-order full CFD estimates quite well. The second-order estimated coefficient does not compare well, and in fact for the pitching moment the trend is not correct. Notice that this grid is much coarser, with only 71,000 grid cells. This trend is continued for the sensitivity to angle of sideslip (Figure 16), which shows a very good comparison for side force and rolling moment, although the comparison for yawing moment is not good at all.

At Mach 1.3 there is only second-order data available (Figure 17 and Figure 18). However, the flow is dominated by the strong bow shock, so flow unsteadiness was less significant. The SA method matches the trend, but not the magnitude of the full CFD data. For minimized-domain predictions, the trend information provided by the SA analysis may be appropriate to reduce the number of CFD evaluations that are required.
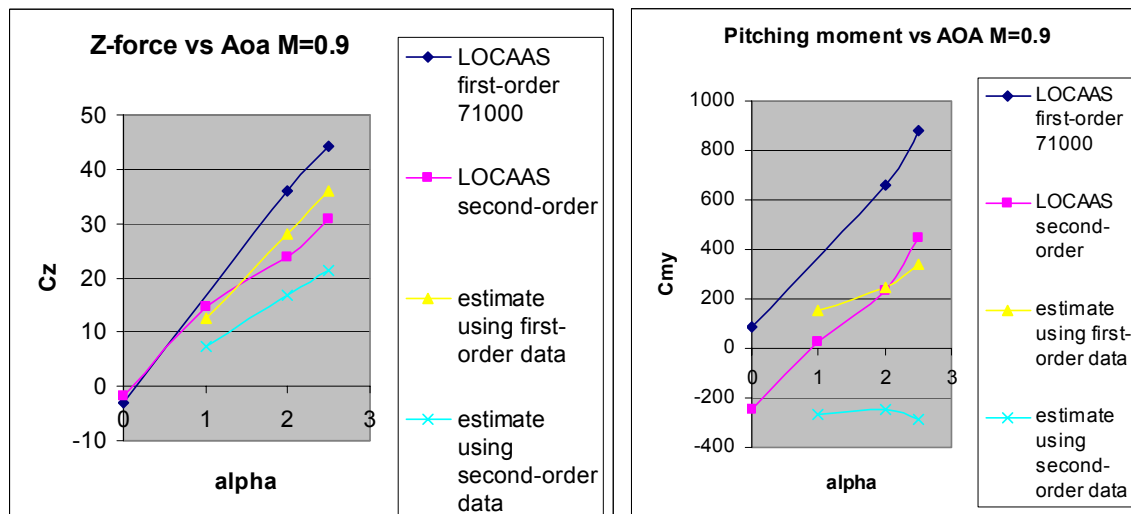

Figure 15: Load coefficient sensitivity with angle of attack, LOCAAS, Mach 0.9
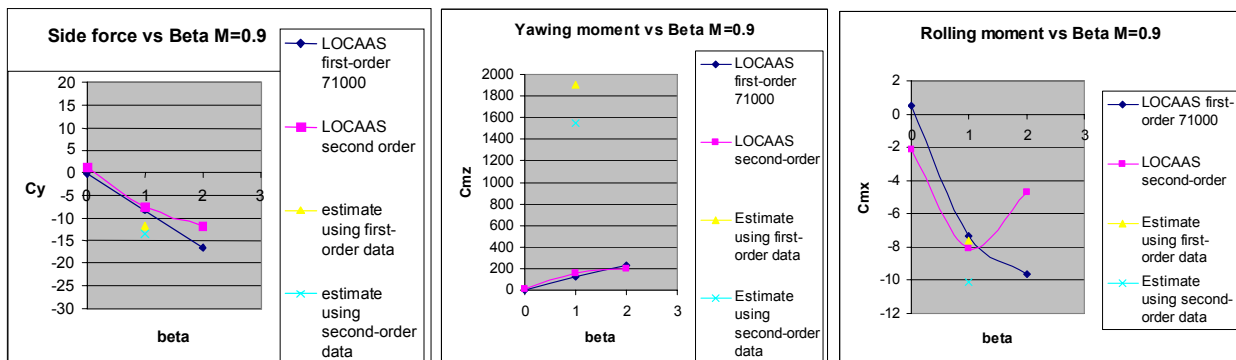
Figure 16: Load coefficient sensitivity with angle of sideslip, LOCAAS, Mach 0.9
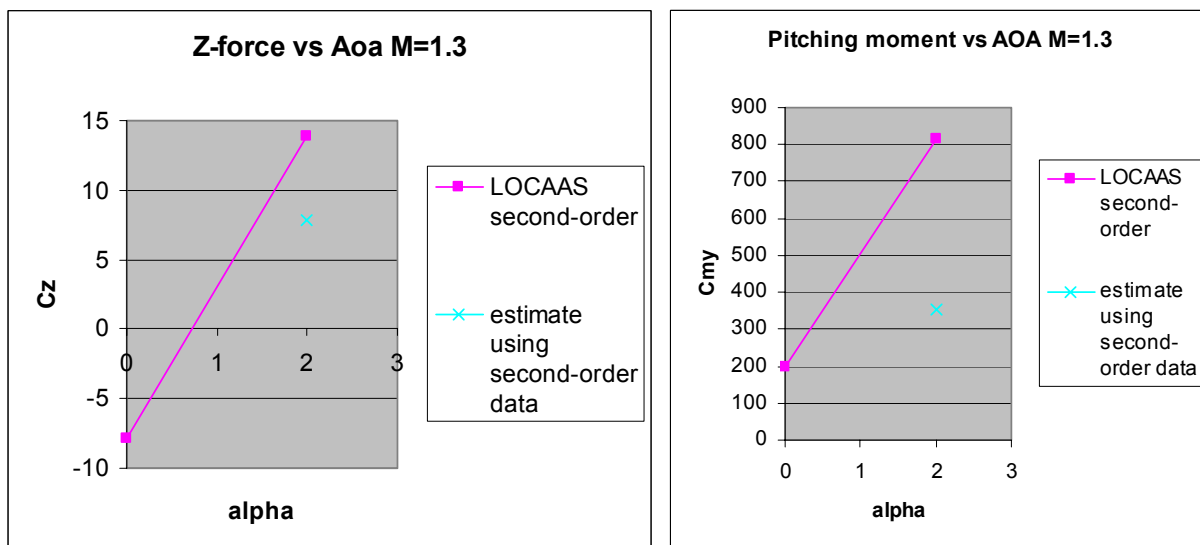

Figure 17: Load coefficient sensitivity with angle of attack, LOCAAS, Mach 1.3
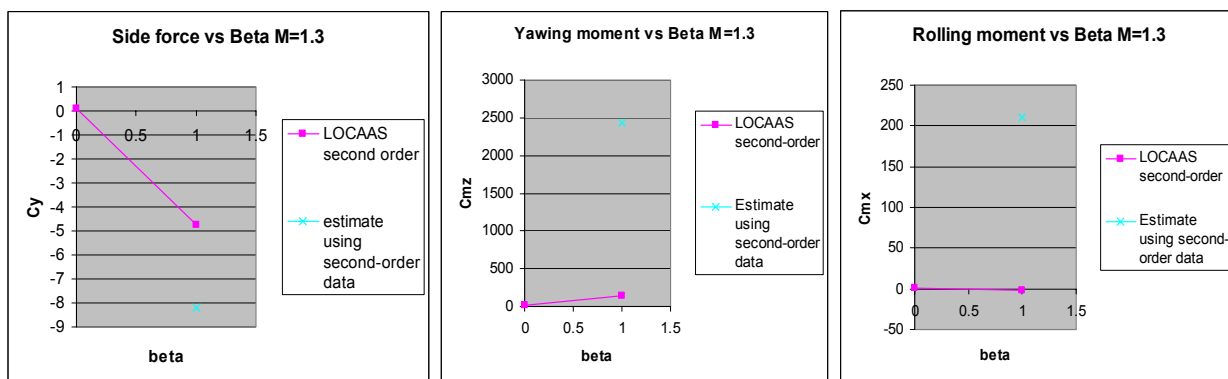

Figure 18: Load coefficient sensitivity with angle of sideslip, LOCAAS, Mach 1.3

4.2.2   MMTD Results

The MMTD with fins deployed is evaluated in the same manner as the PLOCAAS. The perturbations with angle of attack at the two Mach numbers show very similar and expected behavior, with positive perturbation pressures and downward perturbation velocities on the lower surface, and small negative perturbation pressures and downward perturbation velocities on the top surface. Recall that for the LOCAAS, the Mach 1.3 case was much less sensitive to angle of attack. For the MMTD, the shock is attached to the nose, and hence the change in flow is less drastic ahead of the store. The perturbations with angle of sideslip are similar (as they should be, with a symmetric weapon), except for the aft region, which has a fin in the angle of attack case.
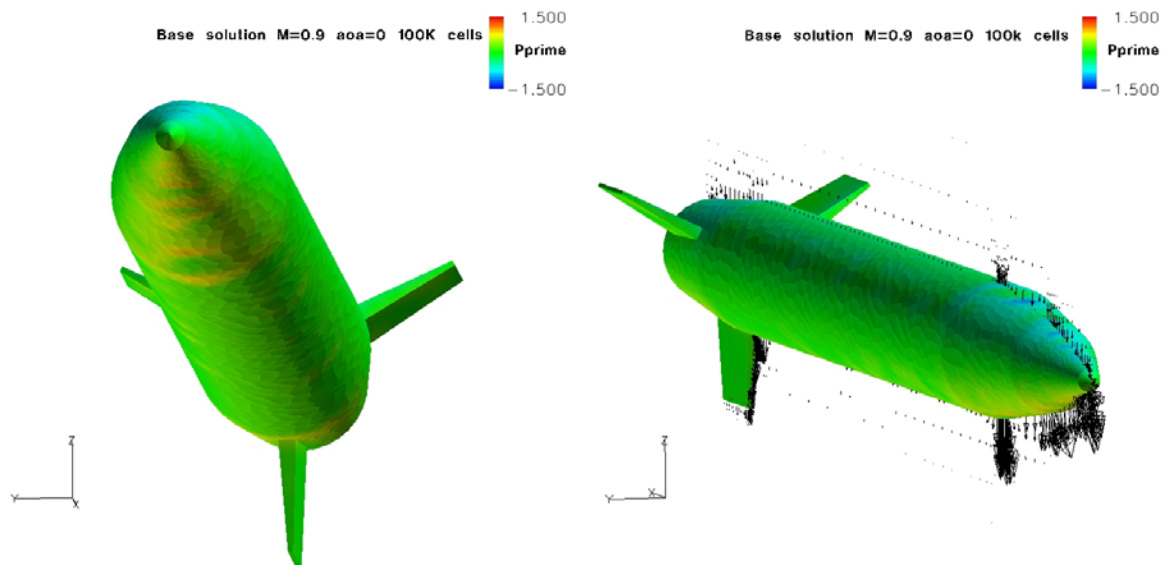

Figure 19: Perturbation pressure and perturbation velocity vectors, MMTD, Mach 0.9, free stream

Store loads were computed using both full CFD (Splitflow) and the SA method. The SA solution at angle of attack or sideslip was computed by multiplying the perturbation solution at each cell center by the selected angle of attack or sideslip and adding it to the base solution at zero orientation, then integrating the resulting surface pressures. The results for the MMTD at Mach 0.9 are shown in Figure 20. The SA solution seems to give the general trend, but the magnitudes of the loads at angle of attack is different for SA and full CFD. The discrepancy between the full CFD results at 100k cells and 190k cells was in all cases within the uncertainty of the experimental data results. Note that the full CFD solution at higher grid resolution gives the wrong trend for pitching moment, more discrepancy than the 0.025 experimental error bar. The pitching moment increments predicted by the SA (x and square symbol) are larger than the magenta line, but by about the error in the experiment. It is also somewhat interesting that the SA-predicted pitching moment using the two different base solutions (computed on different grids) are very close to one another.
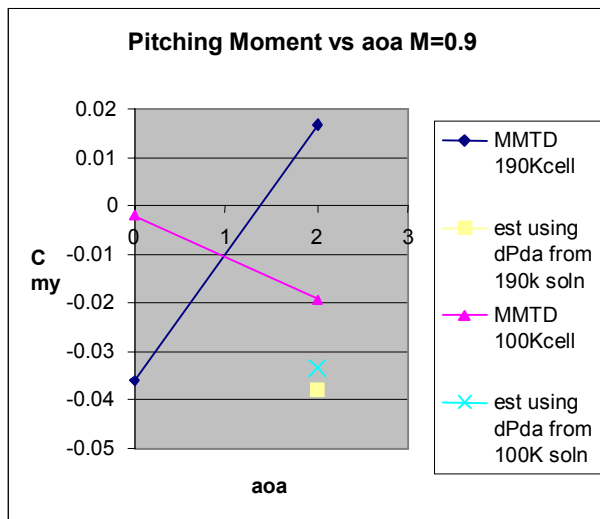
Figure 20: Normal force and pitching moment sensitivity with angle of attack, MMTD, Mach 0.9

The small grid study was done on the MMTD geometry to see if the steadiness of the flowfield had the same effect as for the LOCAAS. Very little difference in the pressure over the surface of the MMTD was found, because the axisymmetric shape of the MMTD inhibits the type of unsteadiness exhibited by the LOCAAS geometry.

4.2.3   Summary of the SA method Results

The SA method with the body rotation boundary conditions clearly captured the trends with variation of angle of attack and sideslip, but missed the actual magnitudes of the coefficients as compared to full CFD. The order of the solution seems to be very important, as the SA method performs better using less refined grids (larger cell sizes, lower solution order) than with more refined grids. This is thought to be a direct result of the unsteadiness of the solution, which is captured with more grid refinement. The more refined cases are capturing a single iterate in a varying solution, and hence the solution is random within some band, whereas the less refined solution is converging more reliably to a steady solution.

5   CONCLUSIONS AND RECOMMENDATIONS

The Minimized Domain CFD (MDCFD) method was evaluated for internal weapons bay release of small, smart weapons. The aircraft selected for evaluation and validation was the F/A-22 with release from the right main weapons bay. The two weapons selected were the MMTD (with fins deployed and retracted) and the LOCAAS tandem configuration. A transonic (Mach 0.9) and a supersonic (Mach 1.3) Mach number were evaluated. For this configuration, the MDCFD method performed as well as for external carriage. The first-order MDCFD computed loads were comparable in accuracy to a full CFD simulation computed first-order. As for external release, there was no real trend to increased accuracy with solver complexity. The average loads computed from the MDCFD second-order simulations were more accurate than the first-order MDCFD loads, and more accurate than the first-order full CFD loads. The average loads computed from fully time-accurate MDCFD simulations had accuracy of the same order as time-warped simulations, and hence were not

worth the added expense. The comparison of MDCFD to wind tunnel data was generally within the error bars of the wind tunnel tests, with some notable exceptions. The normal force and pitching moment data was out of tolerance, but was definitely closer for the second-order simulations. The results of a grid study indicated that the loads calculations were insensitive to the number of grid cells in the 300,000 range, indicating grid independence and adequate grid refinement. The loads were also insensitive to the size of the far field domain, but were sensitive to the size of the near field domain. This is due to the fact that the near field domain needs to contain the unsteady behavior immediately surrounding the bay. The trajectories computed matched in position, but not in angular orientation. The angles were small, however, and the discrepancy is not expected to affect the positional trajectory or predictions of safe separation.

The Sensitivity Analysis (SA) method was implemented in Splitflow and evaluated against full CFD data on the MMTD and PLOCAAS Tandem Pack at Mach numbers of 0.9 and 1.3. The method predicts the expected perturbation of the flowfield with angle of attack and sideslip. The loads computed from the SA method follow the same trends as those computed using full CFD, but the magnitudes at angle of attack or sideslip are much different. The order of accuracy of the solution is critically important, as this affects the unsteadiness of the solution. A steady base solution for the SA method seems to be key to the accuracy of the predicted loads.

6   REFERENCES

[1]   Davis, M.B., Welterlen, T.J., and Corfeld, K.J., "Minimized Domain CFD for Store Separation," AIAA 2003-1245, 41st AIAA Aerospace Sciences Meeting & Exhibit, 6-9 January 2003, Reno, NV.

[2]   Karman, S.L., "SPLITFLOW: A 3D Unstructured Cartesian/Prismatic Grid CFD Code for Complex Geometries", AIAA-95-0343.

[3]   Borggaard, J.T., Burns, J.A., Cliff, E.M., and Gunzburger, M.D., 1993, "Sensitivity calculations for a 2D, inviscid, supersonic forebody problem", *Identification and Control of Systems Governed by Partial Differential Equations*, H.T. Banks *et. al*., ed., SIAM Publications, Philadelphia, PA.

[4]   Reuther, J., Alonso, J.J., and Jameson, A., "Constrained Multipoint Aerodynamic Shape Optimixation using an Adjoint Formulation and Parallel Computers: Part I", *Journal of Aircraft*, 36(1):51-60, 1999.

[5]   Anderson, W.K., Newman, J.C., Whitfield, D.L., Nielsen, E.J., "Sensitivity Analysis for the Navier-Stokes Equations on Unstructured Meshes Using Complex Variables", AIAA 99-3294, Proceedings of the 17th Applied Aerodynamics Conference, 28 June 1999.

[6]   Finley, D.B., Anderson, D.A., thesis to be published.

DISCUSSION EDITING

Paper No. 27: **Relaxed Fidelity CFD Methods Applied to Store Separation Problems**

Authors: Rudy Johnson   M. Bruce Davis   Dennis Finley
Speaker: Rudy Johnson

Discussor: Dr.Koerner

Question: In the past much effort has been invested in the CHIMERA-technique, especially at NASA-Ames and AEDS. How does your CFD-method compare to this? Did you make use of this?

Speaker's Reply: The concept of MDCFD could be easily applied on an oversetgridsystem. It is a complementary approach.
In our implementation we use the splitflow code which is a Cartesian- Local refinement method. The common aspect between MDCFD and overset approaches is the need to interpolate the flowfield at domain boundaries. MDCFD has less stringient requirements on interpolations since we are decoupling the flowfield. Automated interpolation is achieved through use of the fieldview software.

Discussor: Francois Fortin

Question: The first order scheme is very dissipative. The second oreder scheme would be more accurate and would take about the same CPU time.

Speaker's Reply: First order CFD was used to compute the baseline aircraft solution because it converges to a steady solution. We needed a steady solution as a starting point and this was easy. We explored 1st, 2nd order time accurate and 2nd order local time stopping on the MD.

Discussor: A. Cenko

Question: Since we know that Euler solutions can predict trajectories for external stores, but don´t do well for cavity flows, why did you choose the F-22cavity for your evaluation of the minimized domain approach?

Speaker's Reply: The MDCFD approach was demonstrated for external store release and carriage in an AIAA paper at Reno in 2003 (Davis, Waterland). Euler analysis of store separation from weapons bays has been demonstrated in previous efforts and shown to be useful. The authors agree viscous is better, but we must walk before we run.